Fault Diagnostics and Prognostics for Vehicle Springs and Stabilizer Bars

Xinyu Du[1], Lichao Mai[2], and Hossein Sadjadi[3]

[1,2]*General Motors Research & Development, Warren, MI, 48092, USA*
xinyu.du@gm.com
lichao.mai@gmail.com

[3]*General Motors Canadian Technical Center, Markham, Ontario, L3R 4H8, Canada*
hossein.sadjadi@gm.com

ABSTRACT

Vehicle springs and stabilizer bars are critical suspension components impacting vehicle ride and handling experience. Diagnostics and prognostics of springs and stabilizer bars can improve perceived quality, reduce repair cost and increase up-time for fleet vehicles. It's even more important for autonomous vehicles, since there is no human driver to sense the fault symptoms. Currently, there is no production solution to automatically diagnose and prognose spring and stabilizer bar failures, and the existing research work lacks robustness to various noise factors. In this work, a novel solution based on static ramp test is proposed to detect and localize spring and stabilizer bar faults. With limited number of longitudinal and lateral acceleration measurements, the solution can quickly and effectively detect major failure modes, such as broken springs, disconnected stabilizer bars, loose bushing and loose end link. The validation results from a 2017 Chevrolet Bolt EV demonstrate the effectiveness and robustness of the proposed solution.

1. INTRODUCTION

Vehicle suspension generally consists of springs, dampers and stabilizer bars, which allows relative motion between vehicle body and its wheels. The suspension system directly impacts the tire force and suppresses the noise and vibration from the ground. Therefore, it's critical to the vehicle ride and handling experience.

Vehicle suspension system may be damaged or degraded over time. In this work, we focus on the diagnostics and prognostics for springs and stabilizer bars. The damper diagnostics and prognostics will be presented in our

following work. Among all vehicle spring faults, broken spring is a common failure. The broken spring may be caused by corrosion, steel fatigue or structure deformation due to overloading for a long time. The elasticity or length may be changed for a faulty spring, which will result in an unbalanced chassis at each corner, negatively affecting the driving comfort, or even causing damage to chassis linkages.

The most severe failure mode of stabilizer bar is disconnection. When an accident or material fatigue occurs, the stabilizer bar may break, or the end link may disconnect from the joint. In this situation, the stabilizer bar cannot provide necessary torsion force to balance the momentum, which causes more roll angle, and may even lead to a vehicle rollover. Stabilizer bar loose fault, such as loose end link or worn bushing, is more common in the field. The loose end link is shown in the Figure 1. The end link is not firmly attached to the joint, and may slide up and down, when vehicle is turning. It generally makes knocking noise, reduces the handling and increases the roll angle. The worn bushing is shown in Figure 2. If the bushing wears, the stabilizer bar cannot be held firmly in place, and it will slide back and forth. The sliding motion reduces the stabilizer bar's ability and increases the vehicle roll angle.

The spring and stabilizer bar faults are generally caught by drivers during driving. The relative symptoms include excessive chassis bouncing, vehicle sag, especially with full loads, or excessive body roll. During maintenance, spring and stabilizer bar faults can also be noticed by technicians' visual inspections. However, such inspections do take a longer time to complete, and potentially increase the maintenance cost. Therefore, an automatic and accurate diagnostic and prognostic algorithm is needed.

In suspension diagnostics and prognostics, frequency analysis is a common approach. A frequency-based diagnostic solution is proposed using a clustering method (Yin & Huang, 2015). The vibration frequency, peak

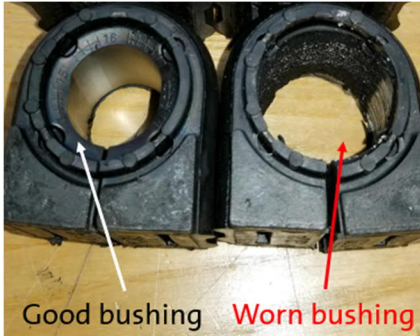Figure 1 Loose end link of stabilizer bar on the vehicle

Figure 2 Worn bushing of stabilizer bar.

amplitude, and relative displacements of a healthy suspension system at four corners are obtained under known external excitation as the baseline. Based on the fuzzy positivistic C-means algorithm and Fisher discriminant analysis, several clusters are found from the data, representing healthy springs. Similarly, the clusters can be obtained from the faulty spring data. Due to the stiffness change, the clusters are different from the baseline clusters. The fault can be detected accordingly. Among the frequency-based diagnostic methods, supervised learning approaches are also proposed (Pravin & Sivakumar, 2019). The vehicle vertical vibration signals are collected from the accelerometer, which is mounted on the top and bottom of each suspension strut. The time-domain data are converted to the frequency domain using Fast Fourier Transform. The spectrum amplitudes are fed into some supervised learning algorithms, *e.g.* SVM, Random Forest, Naïve Bayes, to train a model for fault detection. Frequency analysis of spring resorting force is also employed to detect spring fault (Muhammad & Douglas, 2005). The frequency analysis of vehicle acceleration data is used to characterize suspension response with perturbation. It's discovered that the spring fault causes the changes of frequency characteristics of restoring force, which is used for spring fault detection.

In addition to the frequency-based analysis, physics-based fault diagnostics approach is another route. One proposed diagnostics approach is based on vehicle stability analysis (Zhao & Wang, 2004). It's proved that the vehicle motion is stable for a healthy spring. When the broken spring fault

occurs, the system response becomes chaotic, and the fault can be detected accordingly. Another approach is proposed with dynamics modeling and spring stiffness estimation (Nozaki & Inagaki, 1998). The kinetic vehicle vibration model with two degrees of freedom is developed including the suspension and tires. Based on the equation, the spring stiffness is estimated using the displacement measurement and the tire force estimation. Spring faults are identified by monitoring the spring stiffness change. The machine learning model is employed for spring fault detection along with a physics-based model (Börner, Straky, Weispfenning, & Isermann, 2000). The physics-based model is employed to estimate the spring stiffness. A multi-layer feedforward network is trained to detect the spring fault. The singular perturbation method is also employed to detect suspension faults with multiple operational modes (Luo, Pattipati, Qiao, & Chigusa, 2008). The system excitation under different random load conditions, and their corresponding behaviors (*e.g.* displacements) are measured. The residual of suspension system response is calculated between the baseline healthy data and the test data. The residual above a certain threshold indicates the abnormal behavior in the suspension system.

To the best of our knowledge, there is no paper on stabilizer bar fault detection. None of the approaches described above can isolate these faults. The data used in these approaches are required to be collected during vehicle driving. In practice, the sensor error and environment noises may deteriorate performance. To solve these issues, a robust static ramp test solution is proposed here. The solution is not only able to detect spring and stabilizer bar faults, but also isolate faults to each corner. For the rest of this paper, the proposed solution is described in Section 2, the experiment validation is shown in Section 3, and Section 4 concludes the paper.

2. STATIC RAMP TEST SOLUTION

In this section, a novel diagnostic method using the static ramp test is described. This section includes the theoretical analysis, test setup, data collection, data analysis, and the overall isolation algorithm.

As discussed in Section 1, the degraded or broken springs have significant impact to the chassis and driving safety. If a spring is broken, the chassis height for that corner will be reduced. As shown in Figure 3, it introduces a pitch angle and roll angle for the vehicle.

According to Newton's second law, the acceleration of a vehicle in one direction is proportional to the total external force in that direction, which is shown as: $F = Ma$, where M is the mass of the vehicle, *a* is the acceleration. If the vehicle is in the static condition, *i.e.* the vehicle motion acceleration is 0, the external force is the gravity, and the acceleration is gravity acceleration g. In this condition, the inertia measurement unit (IMU)'s measurements of longitudinal acceleration A_x and lateral acceleration A_y are the

corresponding component of gravitational acceleration due to its working principle. This will directly lead to following equations. In other words, here we're using IMU to measure the pitch and roll angles.

$$Mgsin(p) = MA_x \qquad (1)$$
$$Mgsin(r) = MA_y \qquad (2)$$

where, p is the pitch angle (rotation about y axis), and r is the roll angle (rotation about x axis). x axis is the vehicle longitudinal direction and y axis is the vehicle lateral direction. The above equations can be simplified as below:

$$A_x = gsin(p) \qquad (3)$$
$$A_y = gsin(r) \qquad (4)$$

Through IMU, the longitudinal acceleration A_x and the lateral acceleration A_y can be measured to indicate the pitch or roll of vehicle. For example, on a flat surface, if the front spring is broken, the front corner height will be less than the rear corner height. Therefore, the pitch angle p and the longitudinal acceleration A_x will be negative. If the rear spring is broken, the rear corner height will be less than the front corner height, the pitch angle p and the longitudinal acceleration A_x will be positive. Similarly, the sign of the roll angle r and the lateral acceleration A_y are also correlated. In summary, the longitudinal acceleration A_x and the lateral acceleration A_y are good indicators for broken springs. Please note the pitch and roll angle are also good indicators, but they can't be directly measured from IMU. The average values of A_x for a healthy spring and a broken spring from a 2017 Chevrolet Bolt EV are shown in Figure 4.

In Figure 4, due to instability of the vehicle rear suspension structure, the broken spring is not installed to the rear corners. Instead, three clamps are used to represent the broken spring. Two coils are clamped together by three clamps evenly located at the coil circumference to decrease the coil height. For simplicity, the clamped spring is also noted as the broken spring afterwards. FL and RL stand for the front left and the rear left corners, respectively. The height of bins in the figure
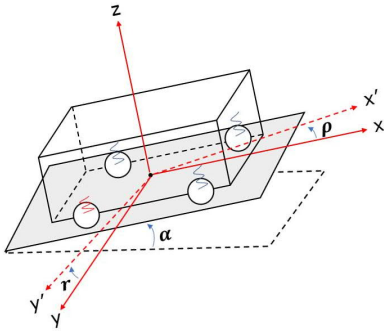

Figure 3. The vehicle with a broken spring on a ramp with grade α (side view). p is the vehicle pitch angle, r is the vehicle roll angle, and x, y, x' and y' are the original and rotated body-fixed axes, respectively, which are defined by Euler angle (Curtis, 2018).

indicates the number of results at certain A_x value, and the fitting curves indicates the distribution of data. It's clearly observed that the front or rear spring faults can be isolated with A_x. Similarly, as shown in Figure 5, the distribution of A_y data indicates the left spring fault can be isolated with A_y from the healthy spring.

Although the average value of A_x and A_y from the test on the level pad can separate the healthy and broken spring, the difference is relatively small and may be affected by measurement errors and noise factors. If the difference of A_x or A_y between a healthy and a broken spring can be amplified, the algorithm robustness will be enhanced. In future, this may also provide the ability to perform early degradation detection. Therefore, our recommended solution is to conduct the tests on a ramp with a known slope angle.

Figure 6 shows a vehicle parked on a ramp with road angle α. The vehicle pitch angle is p. The overall vehicle incline angle
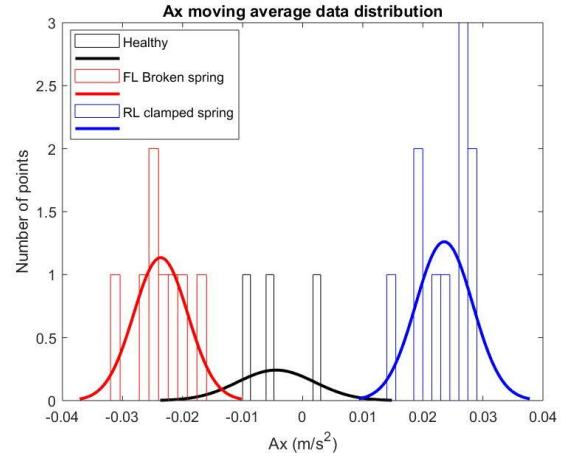

Figure 4. Longitudinal acceleration A_x average value distribution of a healthy or a broken spring on the level pad.
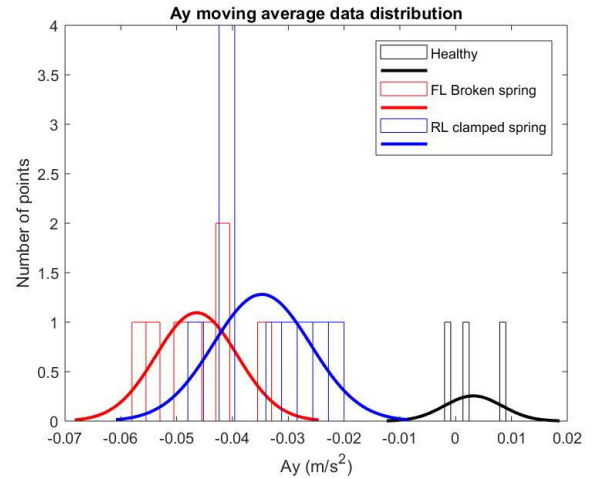

Figure 5. Lateral acceleration A_y average value distribution of a healthy or a broken spring on the level pad.

θ is the sum of the ramp angle and the pitch angle, which is $\theta = p + \alpha$. From the spring perspective, the spring should generate a force to balance the longitudinal component of gravity. The equation can be expressed as follow:

$$mgsin(p + \alpha) = K_p \cdot p \qquad (5)$$

where K_p is the vehicle pitch stiffness. Since the pitch angle p is much smaller than the road ramp angle, the above equation can be simplified as follow:

$$mgsin(\alpha) \approx K_p \cdot p \qquad (6)$$

$$p \approx \frac{mgsin(\alpha)}{K_p} \qquad (7)$$

The pitch angle difference between the healthy and the broken spring can be calculated as:

$$\Delta p = p_{healthy} - p_{faulty}$$

$$= mgsin(\alpha)\left(\frac{1}{K_{p,healthy}} - \frac{1}{K_{p,faulty}}\right) \qquad (8)$$

If the ramp angle α increases, the pitch angle difference Δp also increases, which is good for fault separation. And the longitudinal acceleration A_x is also related to the pitch angle p, which is shown as below:

$$A_x = gsin(p + \alpha)$$

$$= gcos(p)sin(\alpha) + gsin(p)cos(\alpha) \qquad (9)$$

Since the pitch angle p is very small and close to 0, then $sin(p) \approx p$, and $cos(p) \approx 1$. We can simply the equation above as follows:

$$A_x \approx gsin(\alpha) + gcos(\alpha) \cdot p \qquad (10)$$

Then the longitudinal acceleration difference between the healthy and the faulty spring can be expressed as following equations:

$$\Delta A_x \approx gsin(\alpha) + gcos(\alpha) \cdot \Delta p \qquad (11)$$

$$= gsin(\alpha) + mg^2cos(\alpha)sin(\alpha)\left(\frac{1}{K_{p,healthy}} - \frac{1}{K_{p,faulty}}\right)$$

$$= gsin(\alpha) + \frac{1}{2}mg^2sin(2\alpha)\left(\frac{1}{K_{p,healthy}} - \frac{1}{K_{p,faulty}}\right)$$

Hence, a bigger ramp angle will result in a bigger longitudinal acceleration difference ΔA_x, as long as the ramp angle is smaller than 45 degree. In another word, longitudinal acceleration A_x is a good indicator to isolate spring faults.

To validate the ramp effect, several ramp tests are conducted on the level pad (0% grade), 20% grade test hill (11.31 degree in angle) and 30% grade test hill (16.7 degree in angle). Each test data is processed using a 0.2-second moving average

(more details will be discussed in following paragraphs). The distribution of A_x average value is shown in Figure 6.

As shown in Figures 4 and 6, the A_x difference between the healthy and the front rear broken spring becomes larger on 20% and 30% test hills, compared with the data collected on the level pad. It indicates that the ramp can effectively amplify the difference. Similarly, to isolate the healthy and faulty stabilizer bar or isolate the left or right spring fault, the vehicle can be parked across the ramp with left or right side up. When the stabilizer bar fault exists, the roll angle increases, and the measured lateral acceleration A_y can be used to distinguish the healthy and faulty stabilizer bar.

As shown in Figure 7, the data are more separated on the 16% test hill (Figure 7b) than on the level pad (Figure 7a). In another word, the ramp can also effectively amplify the A_y difference between healthy and faulty stabilizer bar condition, because the vehicle has a larger roll angle, when
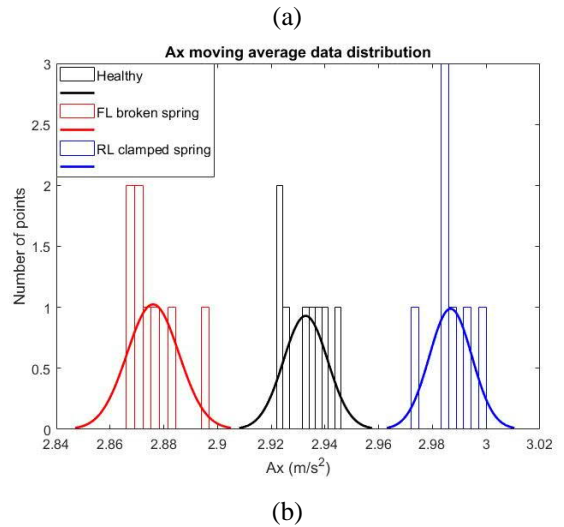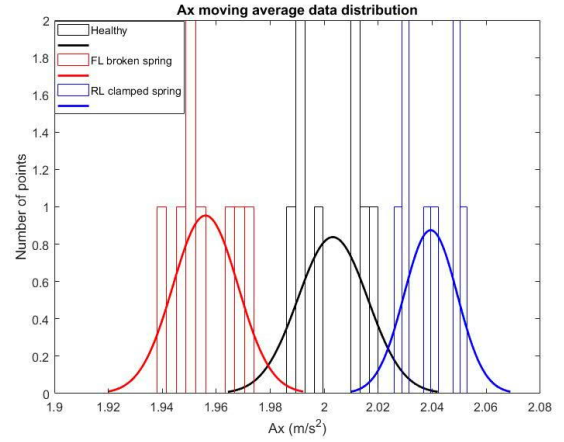

(a)

(b)

Figure 6. A_x average value distribution of a healthy (in black), a front left broken spring (in red), and a RL clamped spring (in blue) on the 20% test hill (a) and 30% test hill (b)
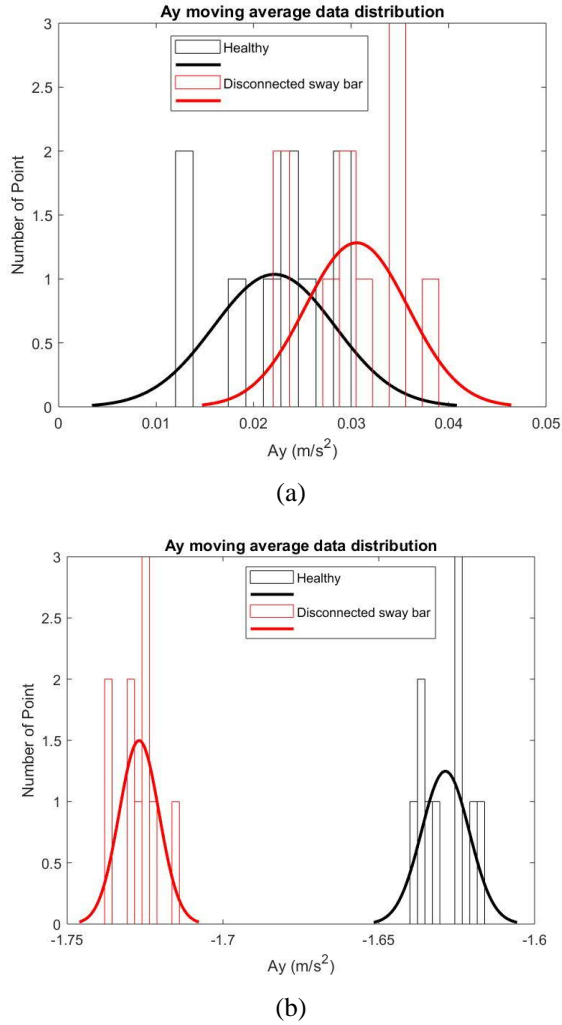
(a)

(b)

Figure 7. A_y average value distribution for healthy (black color) and disconnected stabilizer bar (red color), (a) on level pad, (b) on 16% test hill.

the stabilizer bar is disconnected. Please note that our test ramps for 20% and 30% only have one lane and our test can't be parked left or right side up on these two ramps. Accordingly, the 16% test hill (9.09 degree in angle) is used instead to perform this test. In order to avoid system and measurement error, the measured A_x and A_y data are processed using a moving average filter with the window size of 20, *i.e.* 0.2 seconds data. Please note that the vehicle is standstill, and therefore, A_x and A_y data are almost constant with small variations. The 0.2-second moving average is capable of removing such a variation. The average values of A_x and A_y are used for fault isolation.

With the A_x values for vehicle parking upwards and downwards on 30% test hill, we can detect the front or rear spring fault. Similar approaches can be applied to isolate the spring faults on the left or right side, if we replace the pitch angle by the roll angle, and the longitudinal acceleration by

the lateral acceleration. When the vehicle is parked across the ramp, one side of the vehicle is higher. The broken spring on the left or right side impacts the roll angle and the lateral acceleration A_y.

When the vehicle is parked across on the 16% test hill, the left broken spring causes smaller A_y values, compared with the A_y values in the healthy condition. The right broken spring leads to larger A_y values, because the right corner height is lower, and vehicle has a larger roll angle. If the A_y values are larger than the baseline, *i.e.* healthy spring data, it indicates the right spring fault. If the A_y values are smaller than the baseline, it indicates the left spring faults.

Similarly, when the vehicle is parked across on the 16% test hill with right side up, left side broken spring leads to smaller A_y values, compared with A_y values of healthy condition. The right broken spring leads to larger A_y values, because the right corner height is lower. It's easier to isolate left broken springs from healthy springs than to isolate the right broken springs from healthy springs, when the vehicle is right side up. The right broken springs can be easier isolated from healthy springs, when the vehicle is left side up.

In conclusion, after all measurements on these four vehicle orientations, the spring faults can be determined, and the faults locations can be identified by comparing the A_x and A_y with the corresponding baseline values.

Similarly, the static ramp test can also be used for the diagnostics of stabilizer bar faults. When the vehicle is parked across the ramp, there is a specific roll angle. If the stabilizer bar is loose or disconnected, the vehicle roll angle becomes larger than the angle in the healthy condition. Therefore, the measured A_y will be larger as well. With comparison of measured A_y values, the algorithm can detect the stabilizer bar faults.
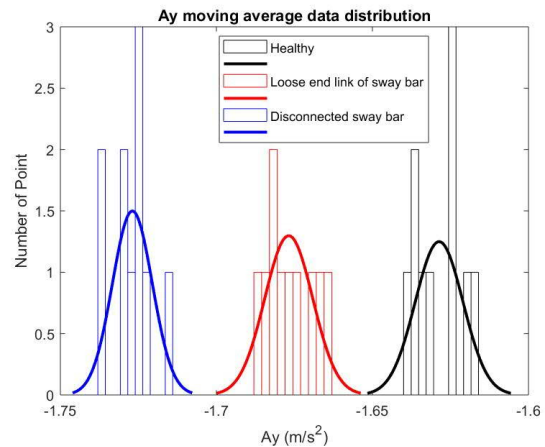
As shown in Figure 8, the healthy, loose end link and

Figure 8. A_y average value distribution of different stabilizer bar conditions (vehicle right side up).

disconnected stabilizer bars can be isolated with the test on 16% hill. The loose end link fault is discussed in the Section 1, and the part is shown in Figure 1. It can also be observed that A_y values for disconnected stabilizer bars deviate more from the baseline than the loose end link fault. The disconnected stabilizer bar can't provide any roll stiffness to the vehicle. Therefore, the deviation is the largest. The loose end link stabilizer bar can provide certain roll stiffness, but not as good as the health stabilizer bar. Therefore, the deviation is less.

To quickly detect and isolate the spring and stabilizer bar fault, a new road test procedure is introduced. The main procedure is shown in Figure 9. There are four places used for static measurements:

Place 1: Vehicle left side up, measure the lateral acceleration A_y

Place 2: Vehicle right side up, measure the lateral acceleration A_y

Place 3: Vehicle front side up, measure the longitudinal acceleration A_x

Place 4: Vehicle rear side up, measure the longitudinal acceleration A_x

The procedure of static ramp test is described as follows,

Step 1: Perform the vehicle check, including tire pressure and vehicle weight, before starting the static ramp test.

Step 2: Slowly drive the vehicle through the places 1 to 4 described as above. The vehicle is parked at each place for at least 10 seconds to collect data, *i.e.* longitudinal acceleration A_x and lateral acceleration A_y.

Step 3: After the test, the fault isolation algorithm (more details are shown in following paragraphs) generates diagnostics and prognostics results.

To generate the diagnostics results, the following static ramp test algorithm is employed, whose flowchart is shown in Figure 10. When the test starts, the buffer is reset, and the parameters are loaded to the algorithm. The vehicle initial condition is checked, including four tires pressures and the vehicle weight. If the tire pressure is more than threshold, *e.g.* 30 psi, and the vehicle weights are smaller than the threshold, *e.g.* 1680 kg, the vehicle is ready for test. If the initial condition doesn't meet the requirement, the tire pressure or the vehicle weight needs to be adjusted.

After the vehicle initial conditions are checked, the vehicle slowly passes through the ramp and the vehicle is stopped at each stop place to complete the static ramp test. When all data are collected, 4 average values of A_x ($A_{x,1}, A_{x,2}, A_{x,3}, A_{x,4}$) and 4 average values of A_y ($A_{y,1}, A_{y,2}, A_{y,3}, A_{y,4}$) are generated. $A_{x,1}$ and $A_{y,1}$ are calculated, when the vehicle left
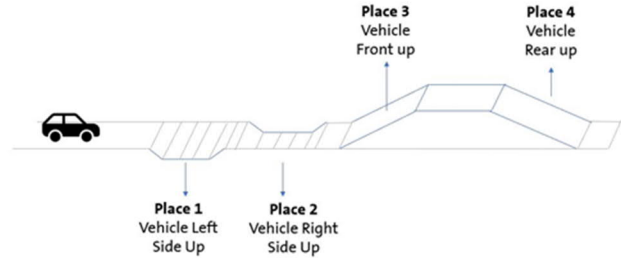

Figure 9. Static ramp test procedure

side is higher. $A_{x,2}$ and $A_{y,2}$ are calculated when the vehicle right side is higher. $A_{x,3}$ and $A_{y,3}$ are calculated, when the vehicle is parked upwards on the ramp and the front side is higher. $A_{x,4}$ and $A_{y,4}$ are calculated when the vehicle is parked downwards on the ramp, and the rear side is higher. All average values are then sent to diagnostics and prognostics blocks. If the minimum tire pressure value is larger than T7, *e.g.* 30 psi, $A_{y,1}$ and $A_{y,2}$ values are firstly loaded to determine the spring condition on the left and right side. If the minimum tire pressure value is smaller than T7, it indicates that the tire pressure is comparatively low and may affect accuracy of the algorithm. If at least one value of $A_{y,1}$ and $A_{y,2}$ is within the threshold, it indicates that the stabilizer bar is healthy, because the faulty stabilizer bar will lead to the increase of the roll angle, and both $A_{y,1}$ and $A_{y,2}$ will be affected as well. The value of threshold T7 will be discussed more in Section 3.

To determine the spring condition, $A_{y,1}$ and $A_{y,2}$ values are compared with the thresholds T1 and T2, respectively. The value of T1 and T2 are calibrated from the healthy and faulty data. They should be calibrated for each vehicle program with different types of suspension or vehicle structure. It's the same for the following thresholds T3 – T6. If $A_{y,1}$ is smaller than T1 and $A_{y,2}$ is larger than T2, it indicates that the springs on the left and right side are healthy. Then the next step Is to determine the front and rear spring. If $A_{y,1}$ and $A_{y,2}$ fails to meet the requirements, it indicates the broken left or right spring, and the further step is needed to isolate the fault location. If $A_{y,1}$ is larger than T1, and $A_{y,2}$ is larger than T2, it indicates the broken spring is on the right side. If $A_{y,1}$ is smaller than T1, and $A_{y,2}$ is smaller than T2, it indicates the broken spring is on the left side.

The broken spring is on the front or rear side will be diagnosed next. The $A_{y,3}$ and $A_{y,4}$ values are compared with T3 and T4, respectively, to determine the fault spring location. If $A_{y,3}$ is larger than T3, it indicates that the broken spring is located on the front side. If $A_{y,4}$ is smaller than T4, then the broken spring is located on the rear side. At the end, the diagnosis results are generated, and the location of the broken spring are listed, such as front left side. In some corner cases, the average values do not meet the above requirements.

The algorithm cannot generate the diagnostic results and will report "unknown diagnostics result".

There are two types of stabilizer bar faults, the loose end link/bushing and disconnected stabilizer bar. Both faults cause the vehicle roll angle increased. To further distinguish these two faults, $A_{y,1}$ and $A_{y,2}$ are loaded to compare with T1, T2, T5 and T6. If $A_{y,1}$ is larger than T5, and $A_{y,2}$ is smaller than T6, it indicates that the vehicle has even more roll angles on both sides, and the algorithm will report "disconnected stabilizer bar" diagnostics result. If $A_{y,1}$ is between T1 and T5, and $A_{y,2}$ is between T2 and T6, the algorithm will report "loose end link of stabilizer bar" diagnostics result.

All diagnostics results and related signal values described above will be saved in the buffer, and eventually reported to the customers.

3. VALIDATION OF THE PROPOSED SOLUTION

To verify the proposed method, some road test data are collected from our test vehicle, 2017 Chevrolet Bolt EV for the different spring and stabilizer bar conditions.

82 road tests are conducted to validate the algorithm, resulting in 80 diagnostics and prognostic decisions. Two tests fail to meet the necessary criteria for fault isolation, and the "unknown" decision is generated. The test results are summarized in Table 1. The performance of algorithm is shown in the confusion matrix, *i.e.* Figure 11.

As shown in Figure 11, the "ground truth" is the actual test vehicle condition, and the "prediction" is the result from the algorithm. The overall accuracy of this algorithm is calculated as the total number of correct results (same as the ground truth) divided by the total number of vehicle tests. The accuracy of the static ramp test algorithm is 97.6%. The false positive rate reflects the percentage of actual healthy cases that are incorrectly identified as faulty cases. The false positive rate of this algorithm is 0. The false negative rate indicates the percentage of actual faulty cases that are incorrectly diagnosed as healthy cases. There are 2 tests of loose stabilizer bars failed to meet the necessary criteria for faults isolation. Accordingly, the false negative rate of this algorithm is 2.4%.

The measurement data A_y for the loose end link and the loose/worn bushing are shown in Figure 12. The A_y measurements of loose/worn bushing condition are different from the healthy condition, and very close to the loose end link of stabilizer bars. Therefore, the algorithm can isolate loose faults from healthy stabilizer bars. Further enhancement of the algorithm and more experiments may be needed if the isolation between the loose bushing faults and the loose end link faults is required. Vehicle tire pressure and vehicle weight are two main noise factors, which may affect the algorithm accuracy. Several tests are conducted using different tire pressures and vehicle weights. The normal tire pressure for Bolt EV is 35 psi. To verify the effect of tire pressure, the tests are conducted with lower tire pressures, ranging from 21 psi to 33 psi. As shown in Figure 13, different tire pressures affect the vehicle corner height, so that the measurements of lateral acceleration A_y are different. Lower tire pressures impact A_y values similar to the broken spring. For example, the low tire pressure at the left side results in a smaller A_y. The summary of road tests with different tire pressures and algorithm results are listed in the Table 2.

As shown in Table 2, true positive results refer to the tests where the algorithm generates the same results as the ground truth. When the tire pressure is lower than 30 psi, some false positive alerts are generated, which incorrectly indicate the broken spring condition. For the tests where tire pressures are 25 psi, 28 psi and 30 psi, the algorithm indicates the "rear left faulty spring". For the tests where the tire pressure of front left tire is 21 psi, the algorithm generates the results indicating the "front left faulty spring". In another word, the low tire pressure will affect the measurements and accuracy of algorithm. To avoid false positive alerts, the tire pressure should be equal or larger than 30 psi, before conducting the test (shown in the fault isolation algorithm on Figure 10). Another robustness test is to increase the vehicle weight and validate if the algorithm will generate false positive alerts. The normal vehicle weight for previous static ramp test is 1600 kg, including one driver and one passenger on the vehicle. In this robustness test, 320 lbs. (145 kg) sandbags are loaded to the rear seats of the vehicle, to simulate the situation of two more passengers on the vehicle. The total vehicle weight is now 1745 kg.

As shown in Figure 14, when the vehicle is parked upwards on the ramp, the larger A_x values are found in the measurements of vehicle with added weight. The algorithm results for these two conditions are listed in Table 3. When the vehicle weight is added to 1745 kg, false positive alerts are generated from the algorithm, which incorrectly report the fault spring condition. To avoid false positive alerts, vehicle weight should be checked before conducting the test. Please note that in the autonomous vehicle setting, where the conditions could be controlled, a single value could be loaded

Table 1. Road test summary

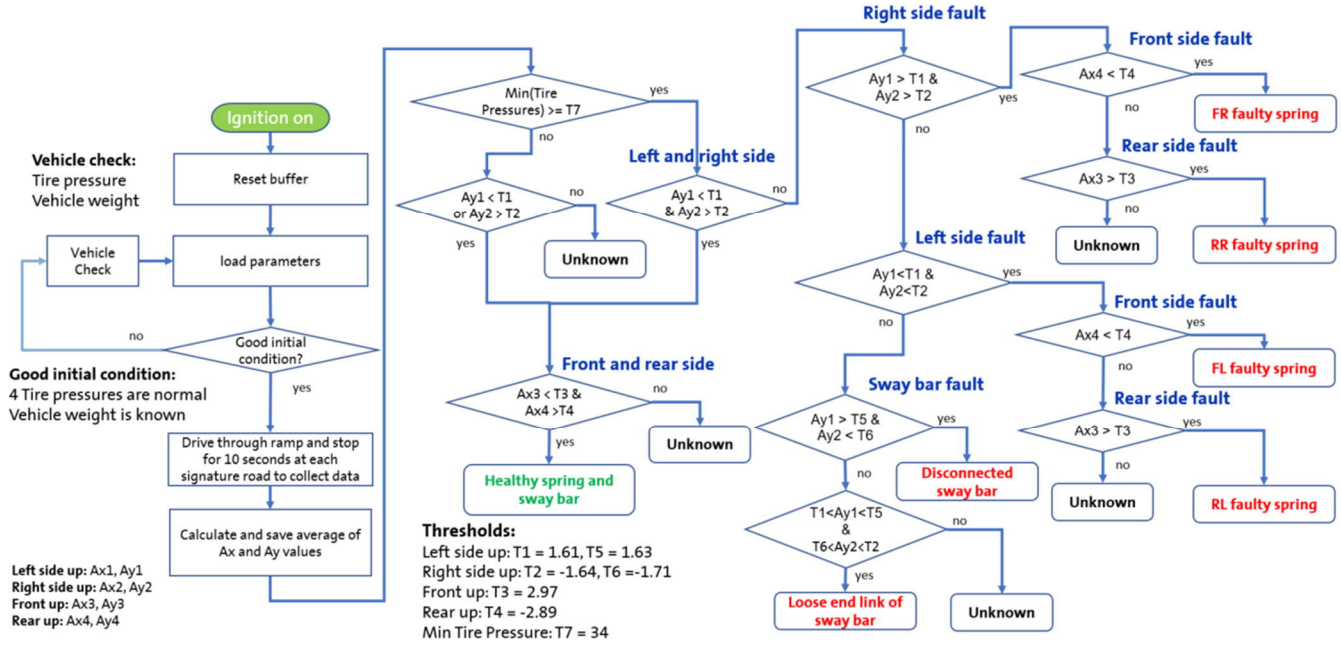| Vehicle condition	Num of tests	Algorithm results
Healthy	28	28
Front left broken spring	8	8
Front right broken spring	8	8
Rear left clamped spring	8	8
Loose stabilizer bars	20	18
Disconnected stabilizer bars	10	10
Total	**82**	**80**

Figure 10. Overall flowchart of spring and stabilizer bar faults isolation algorithm

Table 2. Road test summary with different tire pressure

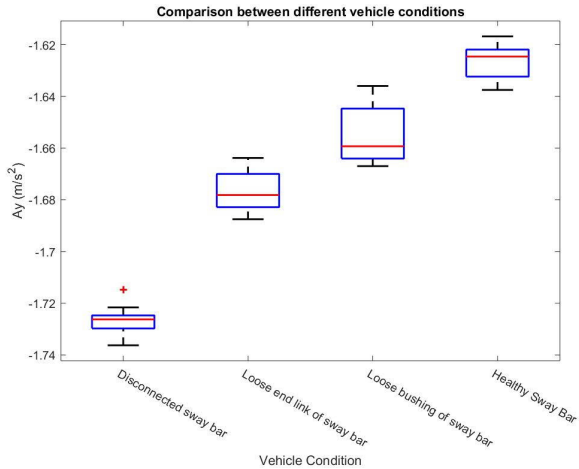| Tire pressure	Num of tests	Num of true positive results	Num of false positive results	Ground truth
Rear Left, 35 psi	8	8	0	Healthy
Rear Left, 33 psi	10	10	0	Healthy
Rear Left, 30 psi	10	10	0	Healthy
Rear Left, 28 psi	10	0	10	Healthy
Rear Left, 25 psi	10	0	10	Healthy
Rear Left, 21 psi	10	0	10	Healthy
Front Left, 21 psi	10	0	10	Healthy

Figure 11. Confusion matrix for the static ramp test algorithm

and not required before each test as long as no passenger is inside the vehicle.

4. CONCLUSION

A novel solution is developed in this work to quickly and accurately detect and isolate spring and stabilizer bar fault. The spring fault can be diagnosed accurately by measuring the longitudinal acceleration and the lateral acceleration of the vehicle on a level pad and ramp, respectively. The stabilizer bar fault can be detected accurately by measuring the lateral acceleration of the vehicle on the ramp. With the proposed solution, the faults of broken spring, disconnected stabilizer bars, loose end link and loose bushing can be detected and localized to each vehicle corner. Based on the 82 road tests with a 2017 Chevrolet Bolt EV, the overall accuracy of the proposed solution is 97.6%. The false positive rate is 0% and the false negative rate is 2.4%. The performance of the solution is impacted by the vehicle weight and the tire pressure. So, the static ramp test should be

8

conducted under predefined conditions, as presented in this report. Such a controlled environment is deemed practical for autonomous vehicle fleet applications. Our future work focus includes the variation analysis between vehicle to vehicle or program to program and modeling for the impact of noise factors.

(a)
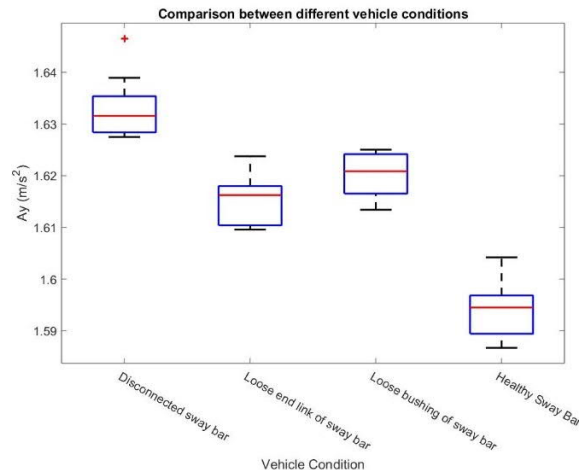
(b)

Figure 12. A_y average value distribution when vehicle is (a) right side up and (b) left side up

Table 3. Road test summary with increased vehicle weight

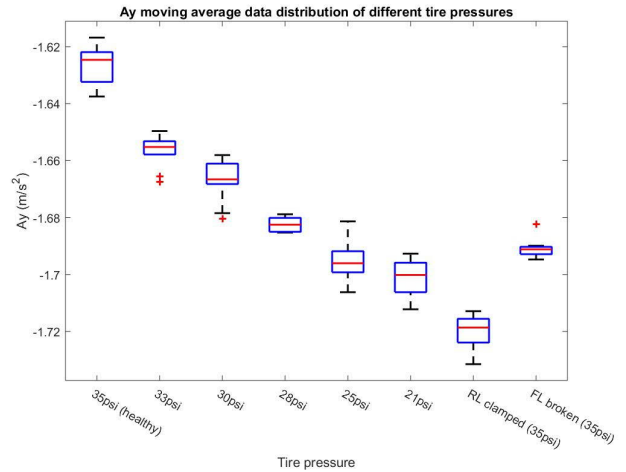| Vehicle weight	Num of tests	Num of true positive results	Num of false positive results	Ground truth
1600 kg	8	8	0	Healthy
1745 kg	8	0	8	Healthy

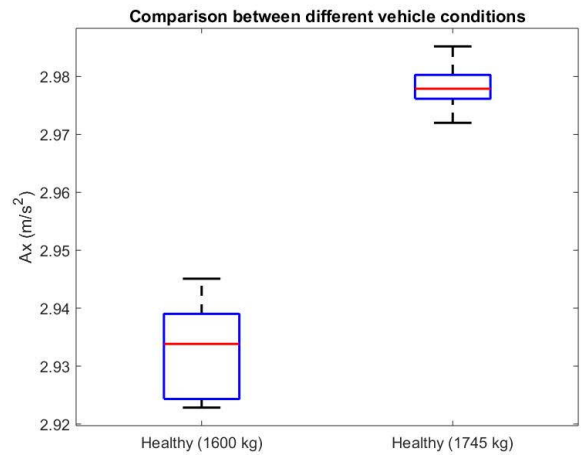Figure 13. A_y average value distribution of different tire pressures

Figure 14. Average A_x distribution for vehicle weights

REFERENCES

Börner, M., Straky, H., Weispfenning, T., & Isermann, R. (2000). Model Based Fault Detection of Vehicle Suspension and Hydraulic Brake Systems. *IFAC Proceedings Volumes, 33*(26), 1073-1078.

Curtis, H. (2018). *Orbital Mechanics for Engineering Students (Fourth Edition).* Waltham, Massachusetts : Butterworth-Heinemann.

Luo, J., Pattipati, K. R., Qiao, L., & Chigusa, S. (2008). Model-Based Prognostic Techniques Applied to a Suspension System. *IEEE Transactions on Systems, Man, and Cybernetics - Part A: Systems and Humans, 38*, 1156-1168.

Muhammad, A., & Douglas, H. E. (2005). Active and Event-Driven Passive Mechanical Fault Identifcation in Ground Vehicle Suspension Systems. *ASME 2005 International Mechanical Engineering Congress and Exposition.* Orlando.

Nozaki, H., & Inagaki, Y. (1998). Measuring and diagnosis technology on shock absorber damping force and coil spring constant, when a shock absorber and coil spring being equipped with a car. *Jidosha Gijutsukai Gakujutsu Koenkai Maezurishu*, 117-120.

Pravin, K., & Sivakumar, B. (2019). Online Model for Suspension Faults Diagnostics Using IoT and Analytics. *International Conference on Advanced Computing, Networking and Informatics.* Indore, India.

Yin, S., & Huang, Z. (2015). Performance Monitoring for Vehicle Suspension System via Fuzzy Positivistic C-Means Clustering Based on Accelerometer Measurements. *IEEE/ASME Transactions on Mechatronics, 20*, 2613-2620.

Zhao, W., & Wang, L. (2004). Nonlinear fault diagnosis on vehicle system in the spring broken down. *Fifth World Congress on Intelligent Control and Automation.* Hangzhou, China.

BIOGRAPHIES

Xinyu Du received B.Sc. and M.Sc. degrees in automation from Tsinghua University, Beijing, China, in 2001 and 2004, respectively, and a Ph.D. in electrical engineering from Wayne State University, MI, USA, in 2012. He has been working at General Motors Global R&D Center, Warren, MI, since 2010, and currently holds the staff researcher position in the vehicle systems research lab. His research interests include fuzzy hybrid system, vehicle health management, deep learning and data analytics. He has published more than 30 peer review papers and holds 33 patents or patent applications. He has been serving as an associate editor for Journal of Intelligent and Fuzzy Systems from 2012 and IEEE Access from 2018. He received the Boss Kettering Award from General Motors for his contribution in integrated starting system prognosis in 2015.

Lichao Mai received dual B.S. degree in automotive engineering from Wuhan University of Technology, Wuhan, China, in 2016, and in mechanical engineering from the University of Missouri, MO, USA, in 2016, respectively. He received a M.S. degree in mechanical engineering from the University of Texas at Austin, TX, USA, in 2018. He has been working at General Motors Global R&D Center, Warren, MI, since 2018. His research interests include vehicle health management, autonomous driving and data analytics.

Hossein Sadjadi received his Ph.D. degree in electrical engineering from Queen's University, Canada, and M.Sc. degree in mechatronics and B.Sc. degree in electrical engineering from the American University of Sharjah, UAE. He has been working at General Motors, Canadian Technical Center, Markham, ON, since 2017, and is currently the Engineering Lead and Feature Owner for Vehicle Health Management. He also had served as a post-doctoral medical robotic researcher at Queen's university, senior automation engineer for industrial Siemens SCADA/DCS solutions, and senior mechatronics specialist at AUS mechatronics center. His research interests include autonomous systems and medical robotics. He has published numerous patents and articles in these areas, featured at IEEE transactions journals, and received several awards.